Integrated geological assessment and numerical simulation for Olkaria's East and Southeast geothermal fields

Bett, Gilbert

Yasuhiro, Fujimitsu
Department of Earth Resources Eng., Faculty of Engineering, Kyushu University

出版情報：Geothermics. 109, pp.102652-, 2023-03. Elsevier
バージョン：
権利関係：

Integrated geological assessment and numerical simulation for Olkaria's East and Southeast geothermal fields

Bett Gilbert[1,3], Fujimitsu Yasuhiro[2]

[1]Graduate School of Eng., Department of Earth Resources Eng., Kyushu University, Fukuoka 819-0395, Japan
[2]Department of Earth Resources Eng., Faculty of Engineering, Kyushu University, Fukuoka 819-0395, Japan
[3]Department of Mining, Materials and Petroleum Eng., Jomo Kenyatta University of Agriculture and Technology, P.o Box 62000, 00200 Nairobi, Kenya

ABSTRACT

Olkaria East and Southeast geothermal fields are located in the East African Rift System and are approximately 120 km from Nairobi, Kenya. It was the first geothermal field in the country to start power production in 1981 Unit I (15 MWe). It has steadily increased its capacity from Olkaria I-VI units to 278.3 MWe (2022). Despite the steady increase in power generation, there has been a notable pressure decline of 10-15 bars. To ensure optimum resource utilization, frequent appraisal is necessary to track productivity and management practices that will guide future investments. Reservoir simulation using TOUGH 2 computational code was employed to assess natural geo-controlling structures for optimal productivity and prediction of future developments in the geothermal field. This study applied the analytical method to determine reservoir rock properties used to construct a conceptual model. The production and reinjection model confirmed declining pressure trends up to 19bars after a period of 29years when1656 t/hr mass is extracted while 42% water reinjection occurs. The extraction of 717.228 t/hr of new wells caused a further decline in production life to 13.48years. This was significant to determine suitable recharge rate, well location and depth interval for reinjection programs to mitigate pressure decline. This study suggested hot and condensate water reinjection of 1530 t/hr (73.62% of extracted fluid) south of Olkaria east field.

1. INTRODUCTION

Olkaria geothermal complex occurs in the depressional basin surrounded by volcanic terrain (escarpments, Eburru hills, Mt. Longonot, Mt. Suswa) in the East African Rift System (EARS), as shown in Fig. 1 (b). The EARS is an intra-continental extensional ridge dotted with soda lakes and active geothermal manifestations (Fig. 1(a)) across Kenya. It has recorded reduced seismicity but with high microearthquake [1] occurrences. In the Olkaria complex, past mapped seismicity coincided with dominant faults, especially NW-SE and NNW-SSE trending faults (Fig. 1 (c)), underlain by three volcanic sequences of 3.5 km thickness [1].

Olkaria geothermal field has multifaceted geophysical structures which act as the impetus for geo-framework for fluid movement that is heated by underlying magma plumes located at about 6-8 km [2]. This includes numerous fault networks, natural water resources and shallow heat sources that create a geo-thermodynamic sequence for geothermal resources. These unique phenomena have supported the huge and rapid expansion of the geothermal field that has contributed immensely to the stable energy supply for Kenya's increasing demand for electricity connections.

The recent expansions in generation capacity from 45 MWe to 185 MWe and the expected production of another unit VI should be monitored and evaluated for the sustainability of present and future investments. The pressure decline of 10-15 bars [3], especially at the center zone of the East field, poses a challenge to further expansion despite the promising reservoir resilience. The significance of this study was to assess reservoir phenomena negated by multiple feed zones of high enthalpy fluid in the shallow and deep reservoir zones.

1.1 Review of Geological parameters

The geological composition of Olkaria's litho-structural units (Fig. 2) resulted from volcanic activities as domiciled by volcanic centers that surround a buried caldera formation referred to as the 'ring structure'. Volcanic rock outcrops (that include comendites, pumice fall, ash deposits, and shooting of trachytic and rhyolitic associated rock types) and pyroclastic sediments occur on Olkaria.

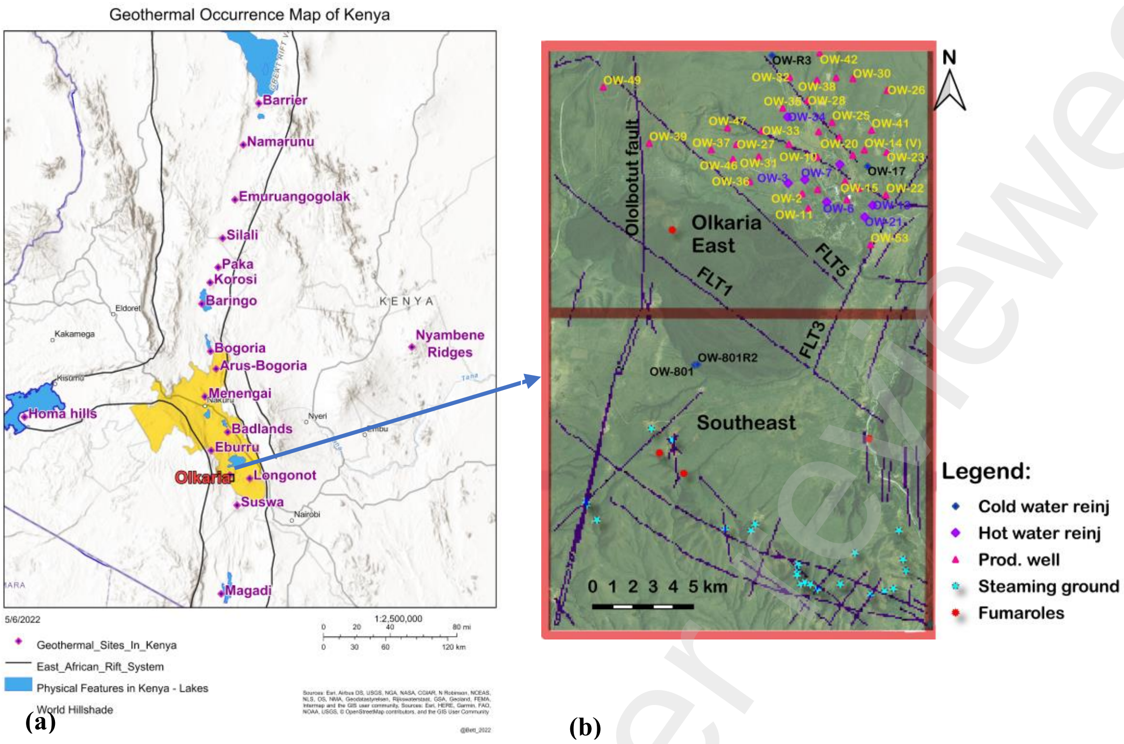

Fig. 1: (a) Geothermal occurrences map of Kenya, (b) and (c) Location and geological features of Olkaria East and Southeast fields.

Normal rifting activities led to faulting including the N-S and NNE-SSW trending faults [4]. The geological structures act as conduits to ease fluid paths in the reservoir rock and allow for fluid-rock interaction.

The main cold recharge faults are the Ol' Njorowa gorge trending E-W system, the Ololbutot fault trending ENE-WSW and the Gorge Farm fault trending NW-SE. Mau escarpment and Lake Naivasha were noted as the primary hydrological sources [5] for aquifer recharge into the reservoirs. Natural water-rock interaction allows for heat exchange through conduction, and subsequently thermal convection in the highly permeable zones of the reservoir. This study targeted the assessment of reservoir extent/ volume, permeability, porosity and rock conductivity, and capacity to sustain increased productivity.

The upward migration of hot fluids is constrained by tuffaceous basaltic caprock that increases in thickness (100-400 m) and depth towards the southeast field due to downthrow influence by surface morphology. The reservoir pore-geometry and connectivity in the trachytic material allow for 5-11% porosity of rock volume.

1.2 Geochemical and geothermometric interpretations

The geothermometer signatures denoted by epidote-actinolite facies [6] indicate high-enthalpies (above 260˚C) in the Olkaria volcanic reservoir domains. Along cold recharge zones, there is a dip (Fig. 3) in the contours due to dilution caused by cold incursion. Thermal boundaries and domains are hydrologically controlled by fluid influxes along fault networks that distinguish the field's productivity, and probably the naming and zoning of Olkaria fields. Wells stratigraphic layout indicates multiple losses of circulation that were coalesced into three main feed zones, namely shallow, intermediate and deep reservoirs, as constructed in the layout below (Fig. 7). The shallow reservoir allows for quick natural recharge along the main aquifers while extensional faults occurring in the deep reservoir segments act as pathways for slow recharge.

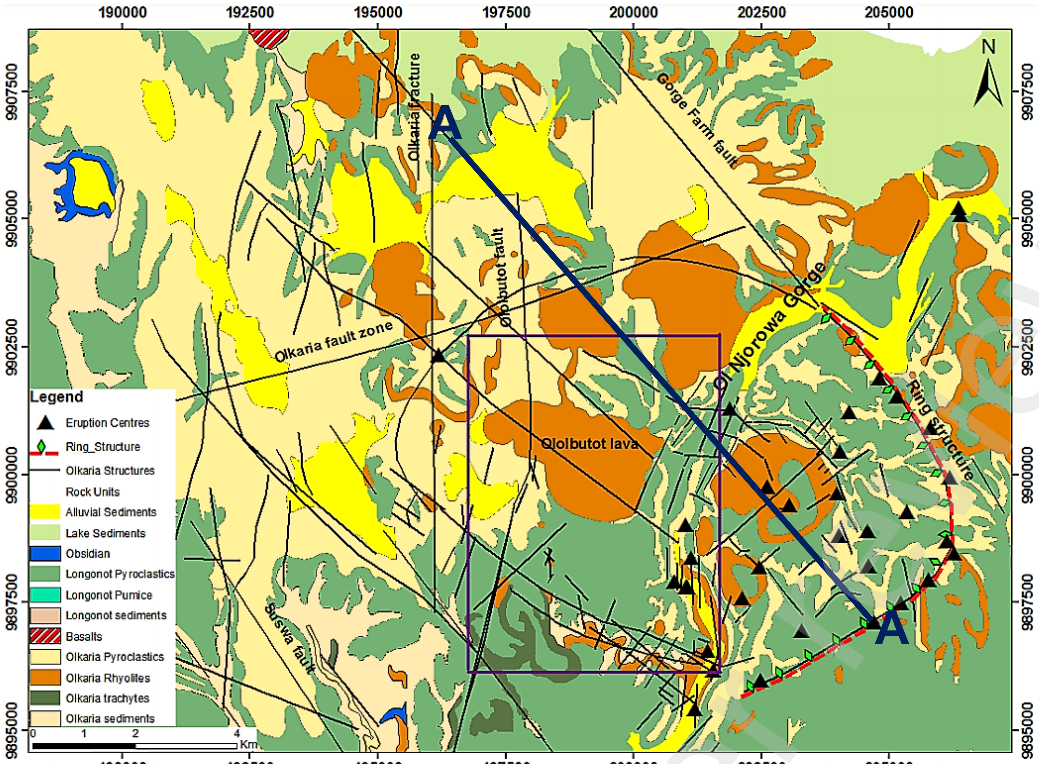

Fig. 2: Surface geological features [7] and location of the study area (purple rectangular shape).

The long-term response to production and reinjection of geothermal systems is controlled by reservoir size, fluid enthalpy, permeability, boundary conditions, and reinjection program. Therefore, pressure decline within the geothermal extraction domain may be out of the reduction of thermal energy or extractable mass.

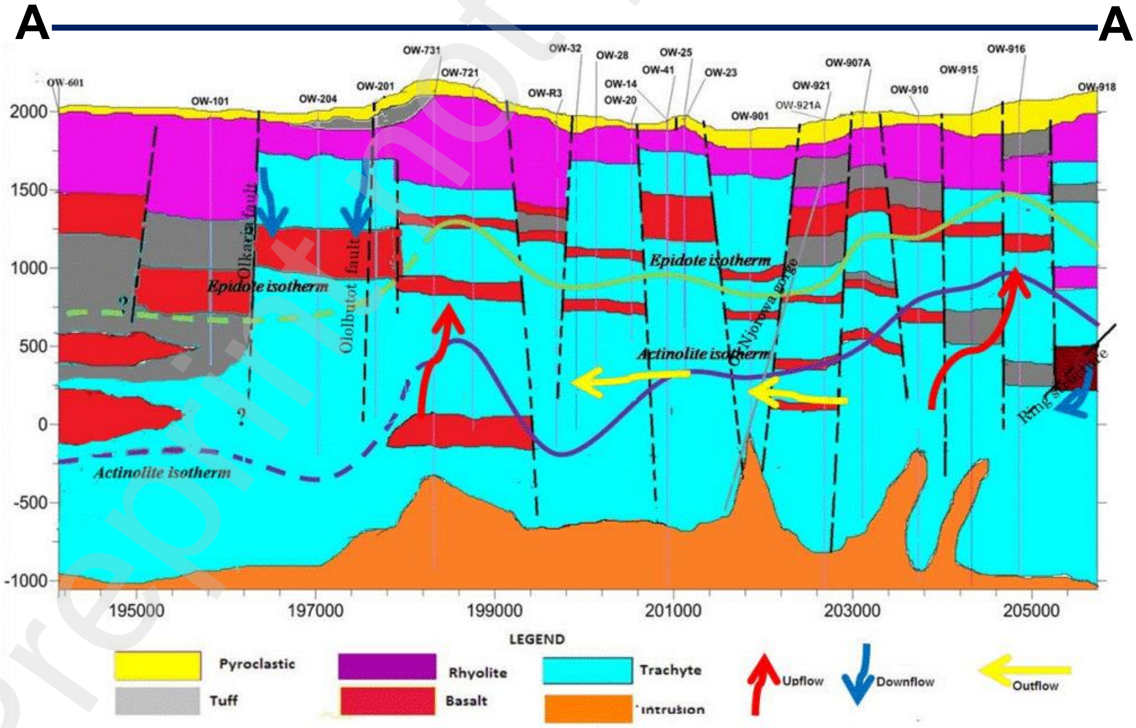

Fig. 3: Lithostratigraphic units and subsurface geochemical facies [8].

Olkaria's geological structure allows for stable inflow of recharge fluid and flow of thermal energy from the conductive body as demonstrated from tracer and interference [9] testing of injectivity and storage capacity. In this case, pressure decline in Olkaria East could have been caused by a lack of reinjection program during the initial stage of production. Therefore, the quick decline in enthalpy and chlorine can be a result of cooling and mixing in the reservoir.

The location and temperature of cold and hot water reinjections contributed to the performance of the neighbouring wells in the field, especially due to interference between wells [10]. In this study, an open boundary condition was assumed to allow connectivity of recharge outside of the field of study.

Olkaria East has recorded reduced productivity in the central zones since most wells, from 31 to 20 wells [11], were either retired or turned into cold or hot reinjection wells. Ouma et al. [9] discussed that OW-18 in the central zone had pressure drawdown of 44 bars and temperature reduction by 4˚C at 1300m by 1999 while the south zone showed temperature inversion at the bottom caused by cold incursion.

In comparison, enthalpy increase (about 600 kJ/Kg) at the central zone compared to reduction (about 400 kJ/kg) at the peripheries of Olkaria East indicates similar trends. The chloride concentration stabilized and recovered (lowered to 300 mg/kg in 1995-1997 [11]) during the trials for reinjection programs (Fig. 4), with fluctuating enthalpies due to cold mass inflow.

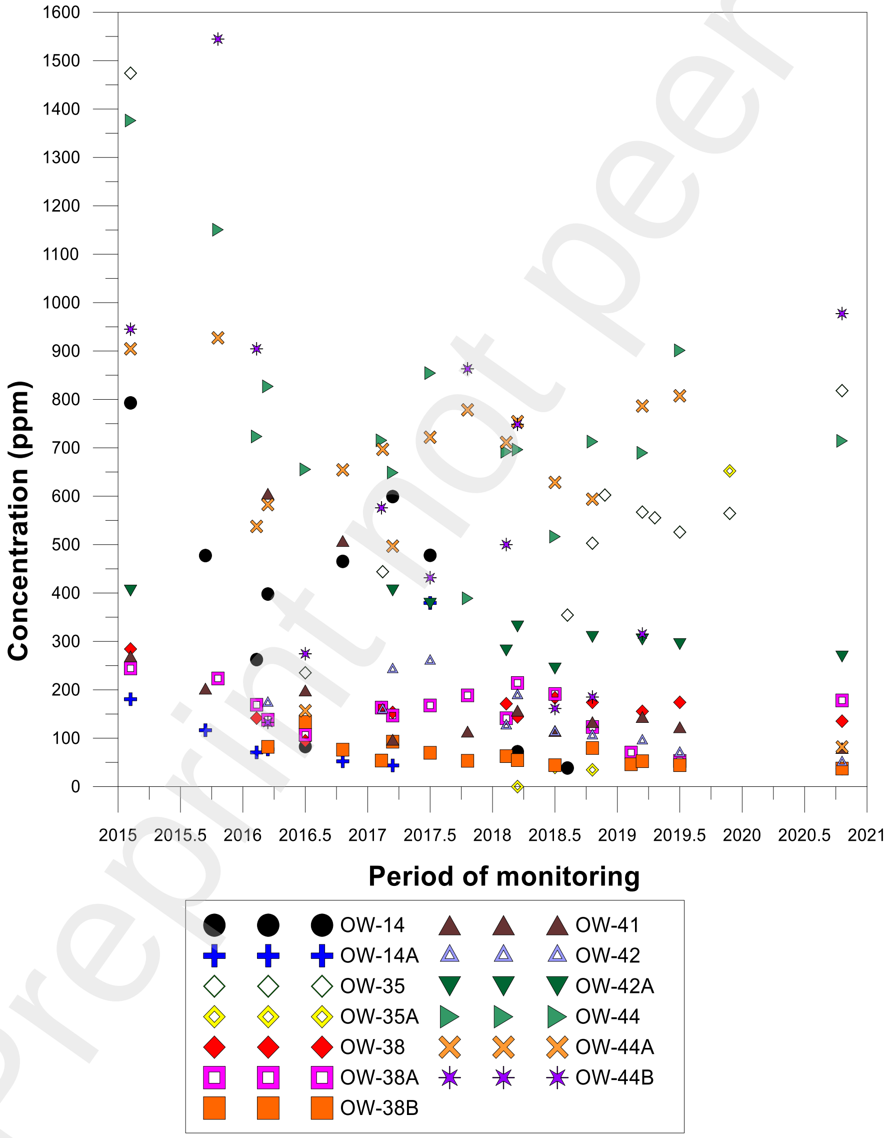

Fig. 4: Chloride evolution from 2015 to 2020

Summary of the reservoir geochemistry for the study area are as follows:

i) The occurrence of boiling effects in the central part of the reservoir is evident with high enthalpies, chloride contents and nitrogen gas concentration.

ii) The solute geothermometry temperatures represent reservoir temperatures of over 300oC (Fig. 5). The fluctuation in some wells is associated with the inflow of cold recharge fluid from neighbouring hot water reinjection.

iii) Dilution processes are also evident as indicated by decreasing trends in the solute concentrations (OW-14 and OW-14A).

iv) Most of the wells assessed in the Olkaria 1AU are currently operating below the minimum silica separation pressures

Southeast field is paradoxically the first explored field yet the least developed due to low enthalpy fluids at OW-01. OW-801-5 series were drilled to intersect the faults (FLT 6-10) in an exploration expedition to determine the reservoir capacity and possibility for future expansion. Therefore, part of this study was to elucidate the reservoir recharge pattern and productivity that support huge surface manifestation (fumaroles and steaming grounds).

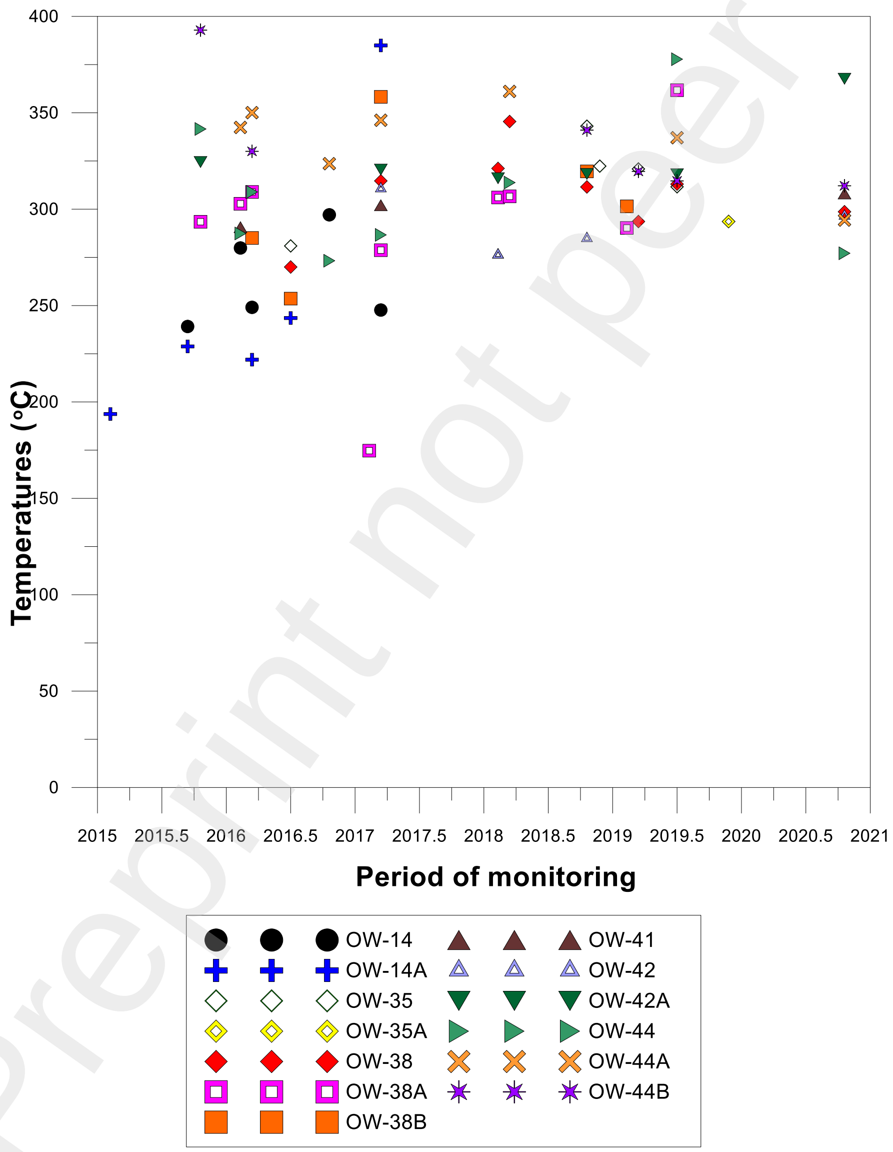

Fig. 5: NaK geothermometer indicates temperature variation with time

Kamila et al. [12] described the sensitivity of enthalpy and energy recovery to different reinjection programs from the periphery to infield reinjection, recharge rate, fluid temperature and depth of reinjection wells. At Olkaria geothermal complex, medium to high enthalpy liquid-dominated fluid of different chemical zone is extracted. Infield reinjection was carried out to mitigate the pressure decline and shallow reservoir boiling. Geological fault network is conduits for inflow whose permeability determines the rechargeability and potential effects in the reservoir. Multiple reservoirs with geological impermeable layers such as in Olkaria will be monitored for their pressure behaviour.

Wang'ombe et al. [14] explain the transmissivity, interference and infield connectivity at Olkaria east central zone by using tracer tests which were carried out by injecting tracer at OW-12. The results portrayed inter-well connectivity between OW-12 and OW-15, OW-16, OW-18 and OW-19. Reservoir response to recharge rate and fault permeability in Olkaria east was examined using the TOUGH 2 code whose method and results are described below.

2. RESERVOIR SIMULATION

In order to understand the resource capacity in the Olkaria field, a numerical simulation [15] technique was used to assess the geophysical parameters and flow of mass and heat that can be extracted. Reservoir simulation was carried out using TOUGH 2 computational code which allows for assessing multi-dimensional fluid and heat flow of multiphase, heterogeneous fluid in porous and fractured media [16]. Input parameters were assigned using pre-and-post processor PETRASIM, which was used to construct the conceptual model as well as portray 3D natural state results. Natural state simulation is the unperturbed assessment of hydrothermal flow regimes in the geothermal reservoir volume using the equation of mass, momentum and energy before exploitation [10].

2.1 Conceptual Model

The conceptual model was constructed using conceptual understanding as follows geological and geophysical [6], [17], [18] attributes and geochemical layout where they described the chlorine concentration and pressure drawdown in Olkaria East wells. The model configuration is illustrated in Fig. 6 below.

Several iterations were run while adjusting the geological properties (including permeabilities and porosities) and boundary conditions for a long simulation time until model stability and convergence occurred.

2.2 Natural State Simulation

The model was simulated on initial boundary conditions where fixed atmospheric conditions (1 bar and 15˚C) were assigned at the top layer while temperature and pressure gradients were 60˚C/km and 1 bar/km, respectively. Ololbotut and George farm faults act as natural aquifers that allowed quick cold recharge into the shallow reservoir (trachytic vein) whereas the bottom layer (syenitic intrusion and basaltic layer) was recharged with 1631.7 kJ/kg. Other parameters assumed in the model include thermal conductivity of 2.0 W/m˚C and specific heat of 1000 J/kg˚C. The model lateral boundary condition was assumed as impermeable and geologically controlled by the extending fault networks, and 500 m buffer zone surrounding the fields. In order to exhibit implicit network rapid fluid flow, faults and segmented reservoirs (Fig. 7) were computed based on the Rayleigh number (R_a) and open aperture (b). Rayleigh number (eq.1) [19] was estimated from 100-1000 for an active geothermal reservoir with formation temperature and pressure gradient to compute the best-scenario reservoir lateral permeabilities (eq.2). Temperature dependence fluid movement in a geothermal convective system has been studied severally [20]–[22].

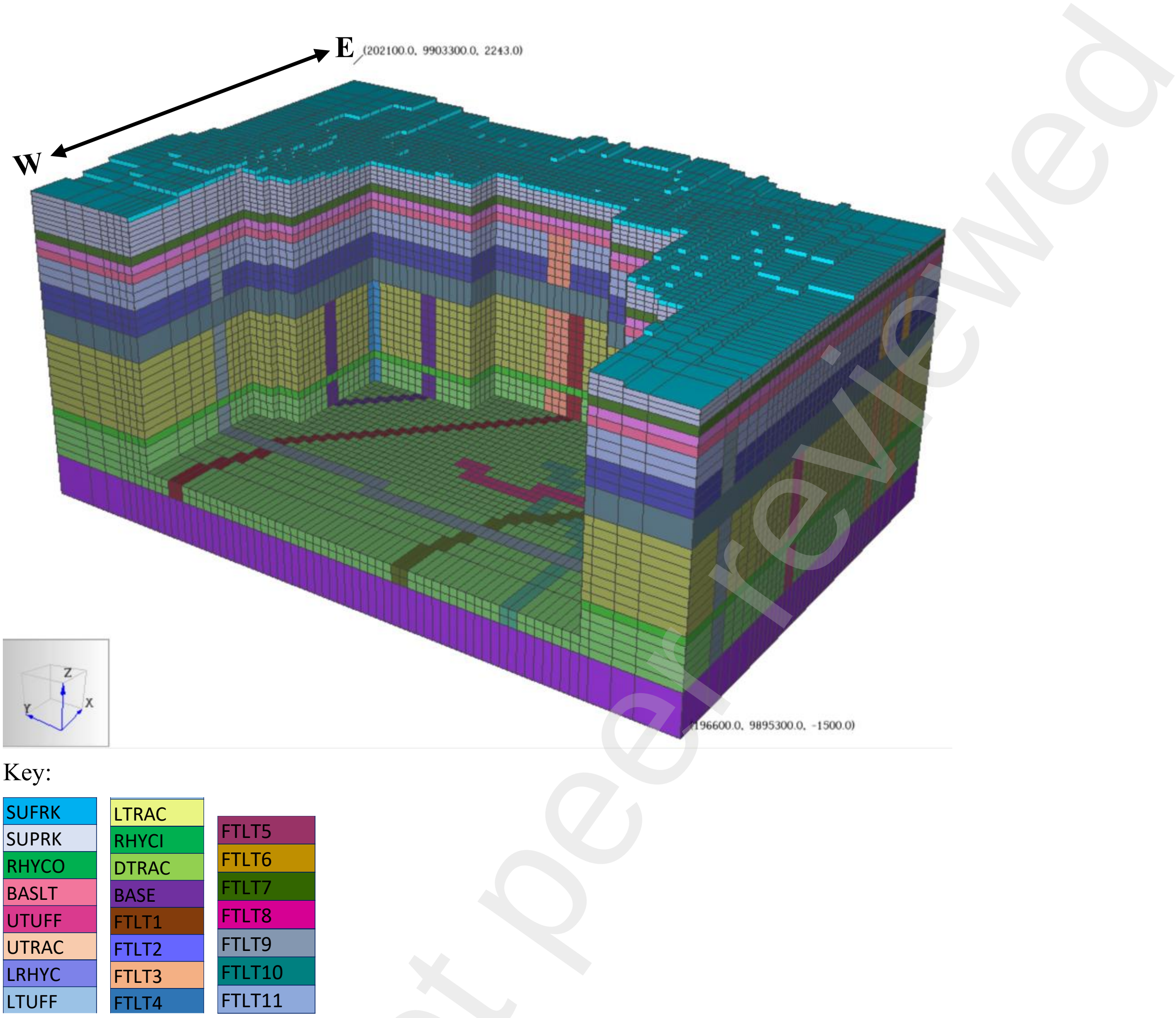

Fig. 6: Spatial distribution of rock types in the conceptual model of the study area

Rayleigh number is influenced by fluid properties such as thermal expansivity β, viscosity λ, and the specific heat capacity of liquid-dominated convective geothermal reservoirs. The kinematic viscosity of brine over such a temperature range decreases while thermal expansivity β increases. The value of the Rayleigh number driven by a relationship of temperature-dependent convective fluid is linearly dependent on β, and inversely dependent on kinetic viscosity [20]. In order to enhance the reliability of the analytical approach and limit the hypothesis discussed by Huang and Wellmann [22] using R_a a stable reservoir rock temperature and two (shallow and deep) confined reservoir scenarios with heat recharge beneath the deep reservoir were assumed. In this case, the dynamic flow occasioned by viscosity-dependent buoyancy effect and lateral thermal expansivity creates a 3D convective domain. The relationship of R_a and Nusselt number was not utilized since the assessment was to understand the lateral porous medium of Olkaria reservoir rock by convection only and R_a >100. Heterogenous and isotropic rock matrices influence the hydrothermal flow of incompressible fluid whose density and kinetic viscosity is temperature driven.

$$R_a = \frac{g\beta\rho_w C_w k h \Delta T}{V_w \lambda} \cong 4\pi^2, \qquad \text{eq. 1}$$

$$\text{Therefore, } k > \frac{R_a V_w \lambda}{g\beta\rho_w C_w h \Delta T}; \qquad \text{eq. 2}$$

Ra ranges from 100-1000 in a geothermal reservoir,

$C_w = \frac{1}{\rho_w}\left(\frac{\partial \rho_w}{\partial P}\right)$ computed fluid compressibility along the saturated curve and pressure gradient (eq. 3) of two-phase fluid.

$$P_{(z)} = P + g\int_{z_0}^{z} \rho_{sat}\, d_z; \qquad \text{eq. 3}$$

Lateral permeability for deep reservoirs ranges from 1-2.5 md whereas shallow reservoir ranges from 3-5 md. Another analytical method was used to estimate structural permeability (and fracture), especially targeting quick cold recharge faults as described in eq.4 below. It is influenced by aperture width and length, temperature-driven viscosity [21], [23] and stable temperature of the two-phase fluid recorded.

$$K = \frac{b^2}{12} \quad \text{, eq. 4}$$

In eq. 4, b represents open fracture; the accuracy of the theoretical value was refined using a lateral relationship of the fluid flow dynamics in the reservoir.

The deep reservoirs have reduced permeabilities compared to the shallow reservoir which illustrates that hydrological flow paths are generally controlled by crisscrossing faults and lineaments beneath the field. This analytic approach coincides with the mapped feed zones as shown in Fig. 7. This was used to constrain the conceptual model and assess the geological properties and extent of the reservoirs.

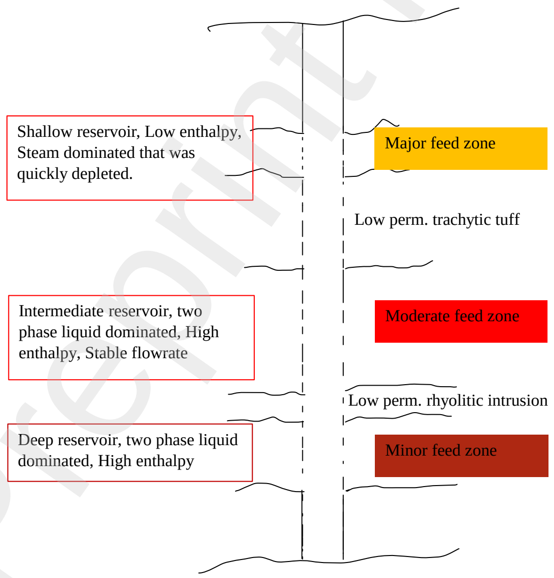

Fig. 7: Sketch for reservoir intersections and depths.

3. RESULTS AND DISCUSSIONS

Simulated results illustrated active geothermal resources that supported the continued field development and further feasibility assessment of the southeast zone. The proximity of deep heat recharge from conductive syenitic-basaltic rock layer and fault-controlled fluid upward trajectory at the East field confirm the geodynamic phenomena that have enabled heat extraction for over 40 years. This occurrence changes towards the southeast field indicated by low enthalpy fluid. However, faults extending towards the East field connect the Southeast with resource recharge potential. Fault FLT1 creates a partial thermal boundary between Olkaria East and Southeast by allowing cold recharge from the Ololbotut fault (FLT9) which thermally affects the SE field.

The representative results below (Fig. 6- Fig. 16) show good matching of measured and simulated temperature and pressure (all are assigned similar styles). Olkaria area is highly faulted which acts as conduits for faster fluid connectivity between cells and encourages huge mass output of high enthalpy brine. Besides the quick recharge along the fractured Ololbotut fault, the rock permeability indices in the reservoir reduce gradually which allows for heat conduction and convection in the deep reservoir. Therefore, wells above and along E-W trending faults were dominated by convective flow. At the shallow reservoir, permeable trachytic material encourages convective and near-isothermal conditions. The basaltic and tuffaceous material contributes to impermeable boundaries that enhance lateral flow and linear geothermal gradient as shown in the temperature profiles.

OW-26, OW-29, OW-32, OW-33, OW-30 and OW-38 (Fig. 8-Fig. 13) were additional wells drilled to tap into the northward hydrothermal flow while OW-47 (Fig. 14) targeted the ENE-WSW fault which supports the productivity among other wells drilled at the central zone that supply steam to Olkaria I powerplants. Cold and hot injection in the East field will reduce reservoir pressure decline and boiling in the central zone of the field. Therefore, despite the reduced mass flow rate in the central zone, the make-up wells at the periphery of the East field (e.g., OW-26 and OW-47) illustrated that natural recharge from Ololbotut and Gorge Farm faults improve reservoir productivity.

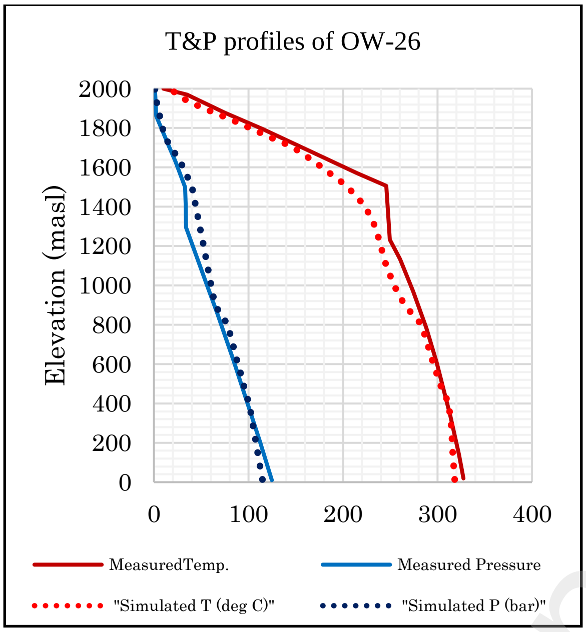

Fig. 8: Temperature and pressure profiles of OW-26

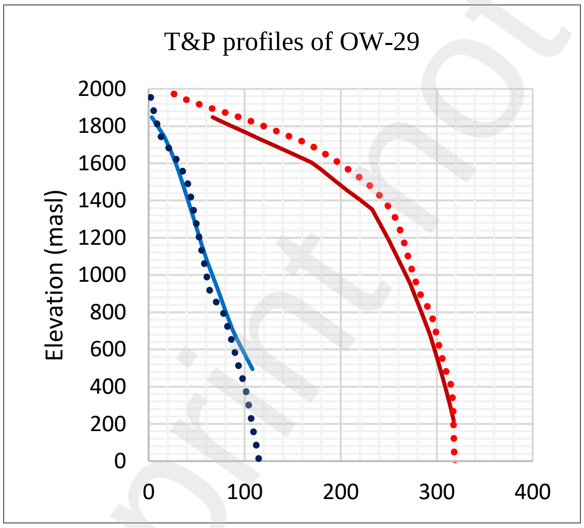

Fig. 9: Temperature and pressure profiles of OW-29

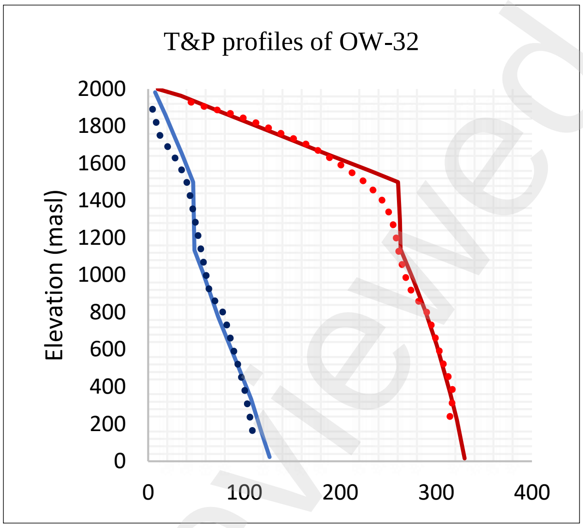

Fig. 10: Temperature and pressure profiles of OW-32

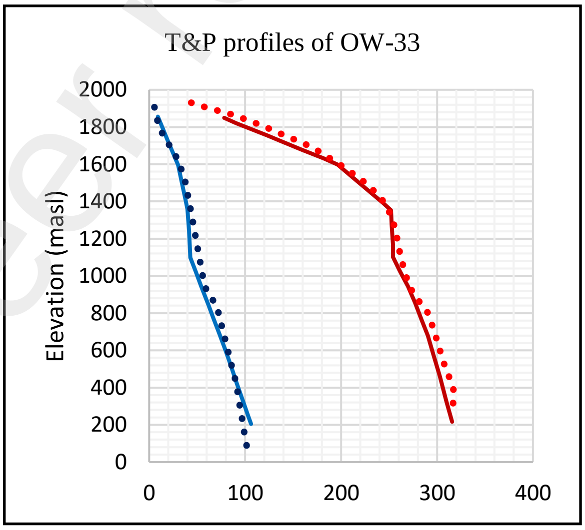

Fig. 11: Temperature and pressure profiles of OW-33

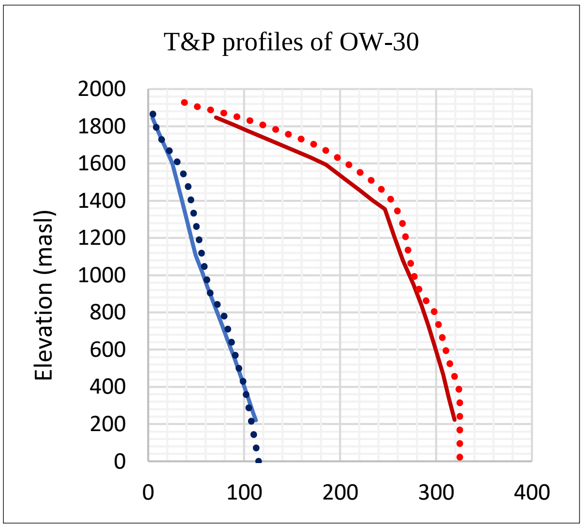

Fig. 12: Temperature and pressure profiles of OW-30

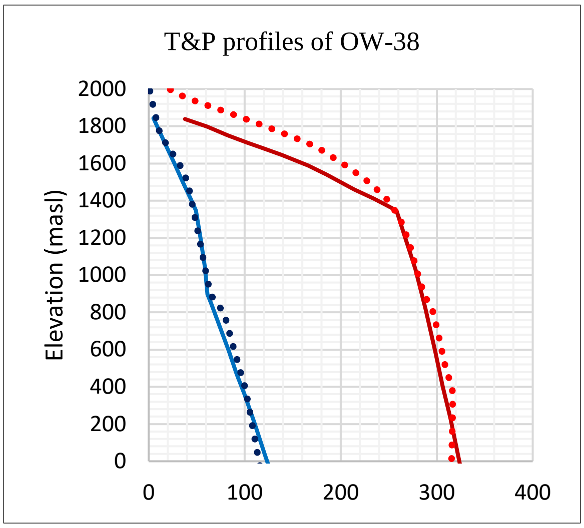

Fig. 13: Temperature and pressure profiles of OW-38

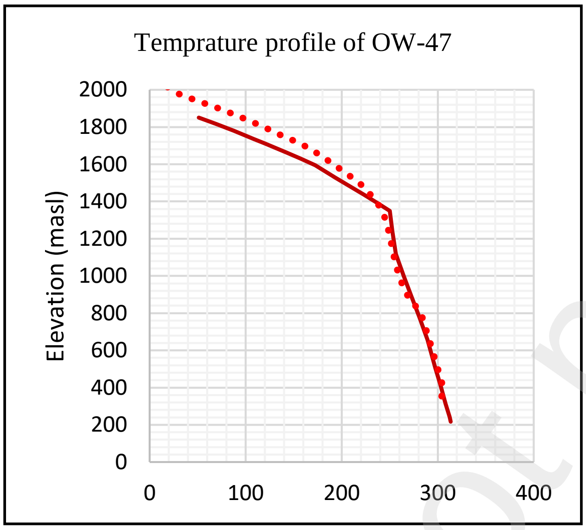

Fig. 14: Temperature profiles of OW-47

OW-803 and OW-805 wells (Fig. 15-Fig. 16) occur in the SE region where a swarm of fissures (Fig. 1(c)) supports high-pressure domains but low enthalpy fluid flow. Ololbotut fault plays a significant role in natural recharge which alongside the proximity of the heat source contribute to a low-temperature gradient. Therefore, the pressure gradient in these wells was attributed to volumetric hydrothermal flow due to the mixing of cold and hot fluid.

The steady-state model illustrates the natural flow both through conduction and convection especially at impermeable rock matrices and fault-controlled fluid flow respectively.

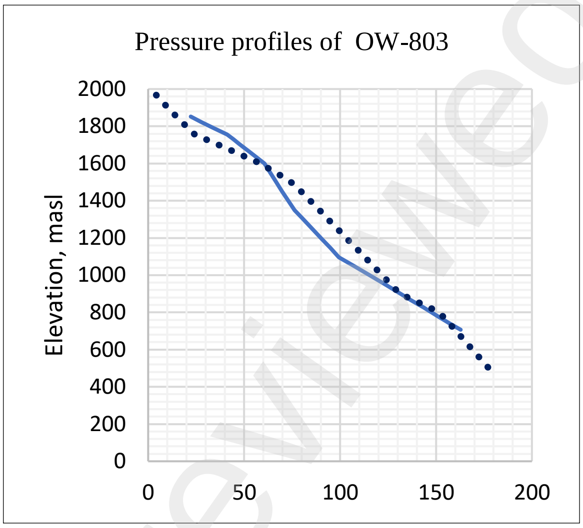

Fig. 15: Pressure profiles of OW-803

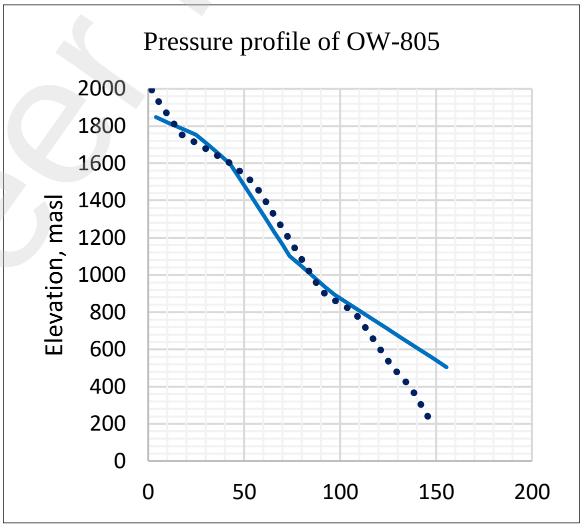

Fig. 16: Pressure profiles of OW-805

Geothermal productivity occurrence increases towards the heat recharge zone, which supports clustered productions wells in the East field (Fig. 1(b)), which decline along natural cold recharge (Fig. 17(a)) whereas surface manifestation occurs along the Ololbotut fault and low enthalpy zones (SE field: OW-804, OW-805). The distinct high enthalpy fluid at the east field shows conductive and convective thermodynamic heating occurrences from deep magmatic intrusive rocks that influence reservoir productivity compared to the southeast where lateral hydrothermal flow act as heat recharge.

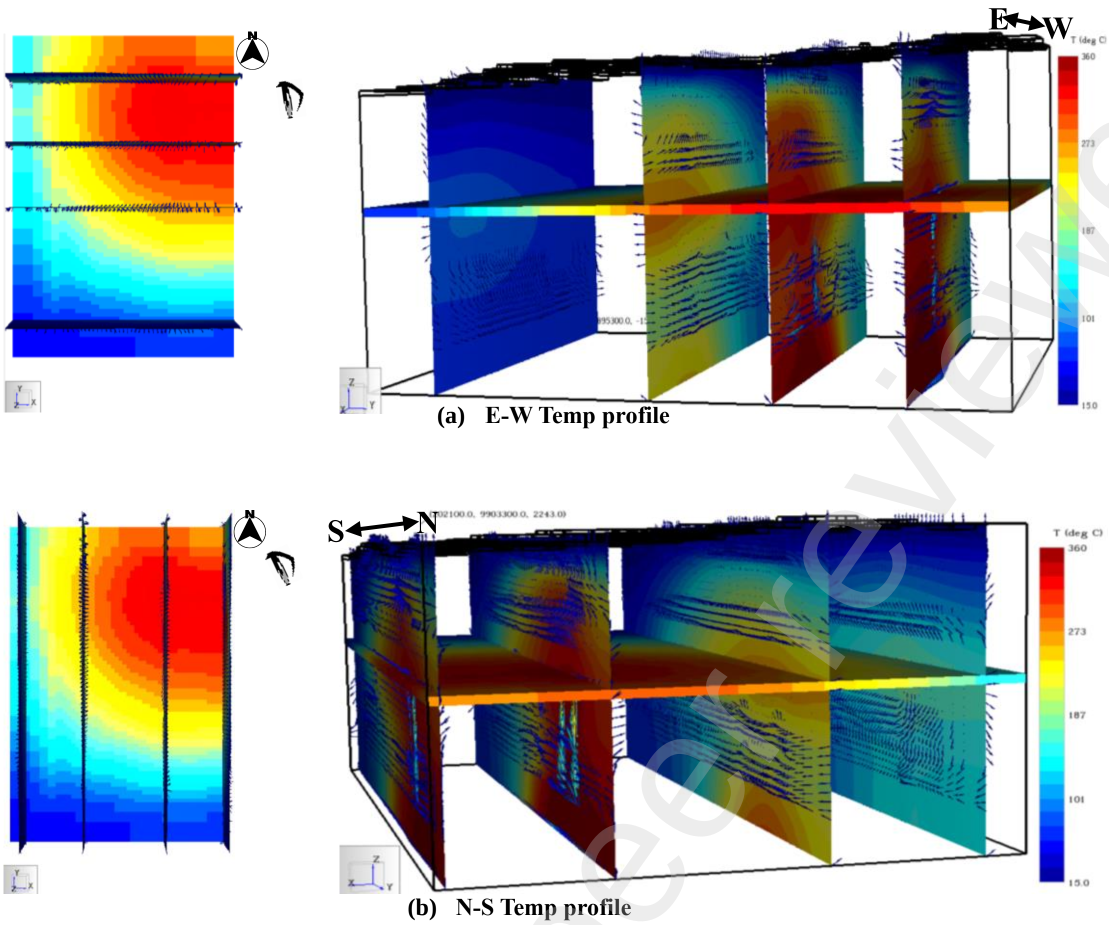

Fig. 17: 3D natural simulation results show temperature distribution at **(a)** E-W and **(b)** N-S

The rate and temperature of cold inflow from recharge fluid create thermal boundaries of hot and cold zones. The natural recharge along the Ololbotut fault separates the East and West Olkaria geothermal fields. Deeper structures allow for connectivity (Fig. 17(b)) due to the permeability of the trachytic rocks. Since N-S trending faults provide high transmissivity, exchanges of thermal fluid between East and West zones could be minimized. The subsequent assessment of production and reinjection in the study area investigated the influence of the pressure decline trends and reinjection programs employed. The reduction in reservoir pressure during the initial production (the 1980s) of the Olkaria East field was influenced by the mass production that decreased the fluid ratio in the reservoir. This was also noted due to boiling in the shallow reservoir as discussed by Ofwona [3]. In addition, without reinjection, the field became susceptible to pressure and mass flowrate fluctuations due to the volumetric imbalance as also indicated by chloride concentration. Hot (reinjected water) and cold injections generally contribute to mass balance, but reservoir pressure is not yet recovered as previously predicted [3]. It is also worth noting that the increase in mass extraction at Olkaria east to supply steam to new power plants may have affected the prognosis results. Continuous monitoring and evaluation help to understand the nature of reservoir dynamism as fluid is extracted and re-injected into the reservoir.

The Southeast field has a huge surface manifestation but a colder deep reservoir due to the proximity of heat recharge as described by Mariita [2]. Several fissures and faults guide fluid to the shallow depths and enhance thermal alteration and support fumaroles. However, mass balance occurs due to recharge from Ololbotut and George firm faults.

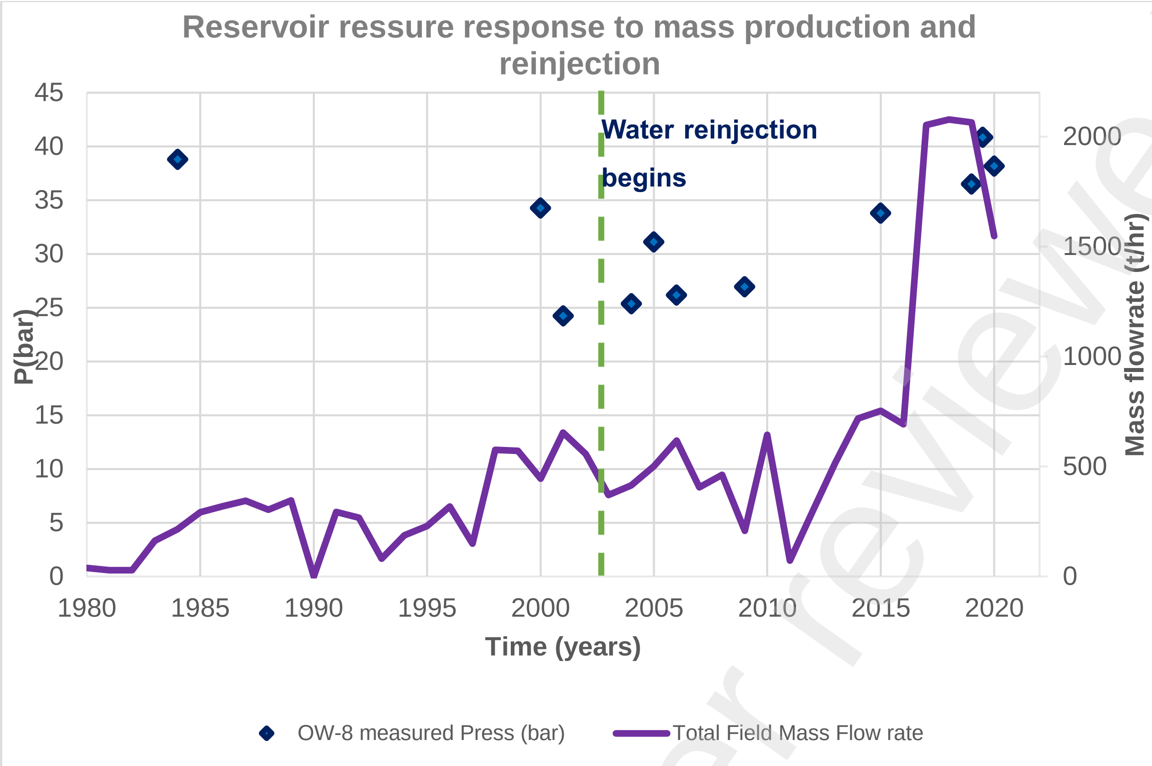

Fig. 18: Reservoir pressure response to mass production and reinjection

Infield reinjection was launched in 2003 after attempts to understand the extent of reservoir response. As portrayed in Fig. 18 the pressure increase was observed which was mirrored by chemical changes (Fig. *4*) in the reservoir fluid. Mass extraction has been supported by make-up wells drilled to counter the declining steam supply.

This is both reservoir management and an economical challenge due to the financial and logistical requirements which prompted the case studies to assess the best scenario for reinjection programs. Hot water reinjection at the central zone creates pressure difference zones (Fig. 19 (a)) which extend southwards following highly permeable fault structures. This was also influenced by continued production where pressure trajectory increases at deeper reservoirs where reinjected fluid also occurs. Lateral hydrothermal flow increases as the fluid rise to shallow reservoirs (Fig. 19 (b)-(c)) and encounters cold fluid which created convective cells. The rate of hydrothermal is demonstrated by vector volume and directions within the domains of fluid interactions.

The study assumed water reinjection of an average rate of 19.44 kg/s (case I) where the hot (separator) water was reinjected at the OW-6, OW-7, OW-12, OW-13, OW-21 and OW-34 of enthalpies 727.336 KJ/kg and condensate reinjection at OW-17, OW-801 and OW-801R2 with fluid enthalpies of 567.23 KJ/kg and 432.16 KJ/kg, respectively. Case II, IB has nil and average 10.444 kg/s reinjection fluid, respectively. Case III assumed similar parameters as the case I except that OW-34 was suspended.

Fig. 20 below illustrates the effect of reinjected fluid on the production life of the geothermal model. Increasing reinjected amount does not automatically expand the production duration but also the location and enthalpies of the reinjected fluid. Make-up wells allowed for future fluid extraction.

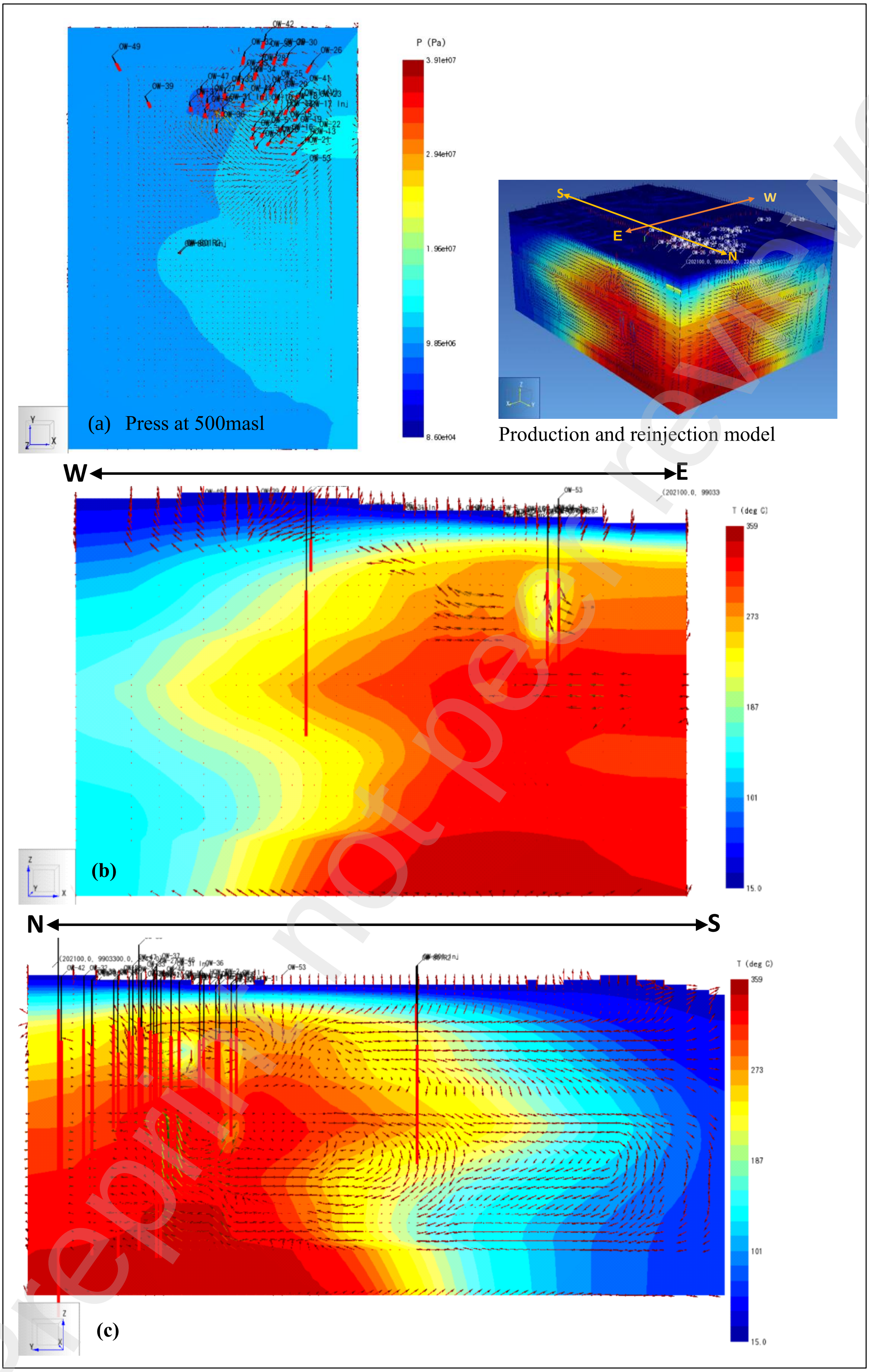

Fig. 19: XYZ slices of production and reinjection model; (a) pressure regimes at 500masl, (b) E-W and (c) N-S hydrothermal flow. Vector arrows indicate the fluid flow paths.

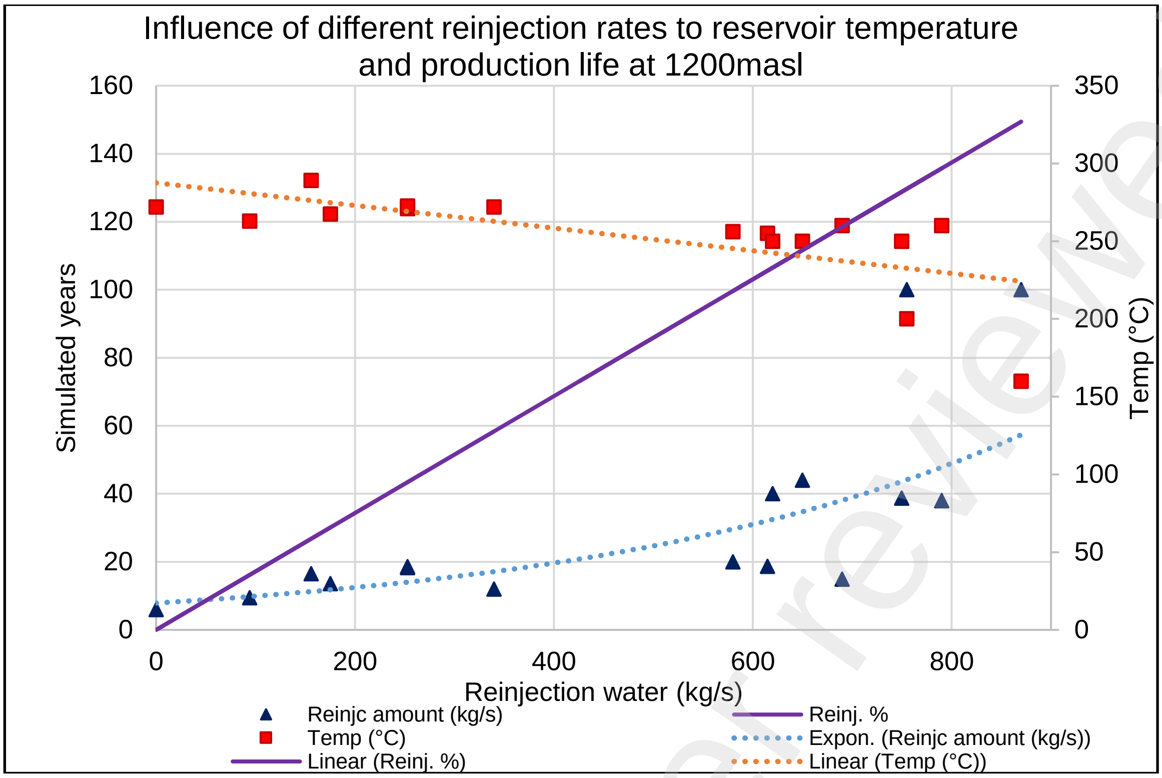

Fig. 20: Reservoir response due to different reinjection.

Assuming the above reinjection programs but lowering the completion depths (600mals and then 0masl) allowed for regaining of pressure changes curves at the shallow reservoir to the formation pressures but a decline of reservoir temperatures at about 500masl from 320°C to 300°C. The simulation years increased to a maximum of 139.38years for the 425 kg/s (case XXIIIB) reinjected fluid along FLT1 and Southeast field (Fig. 21) which allows mass balance with extracted fluid.

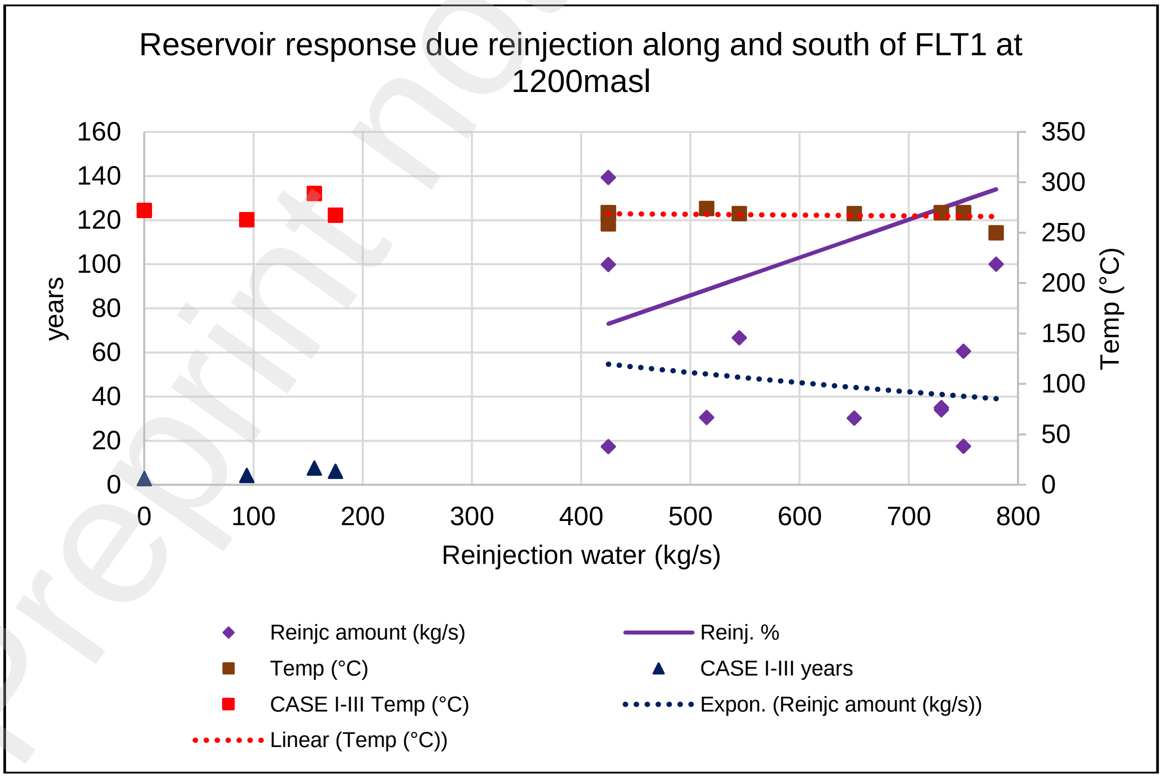

Fig. 21: Reservoir response due to reinjection along and south of FLT1.

Reservoir monitoring was carried out in OW-8, OW-34 and OW-4, to assess the Olkaria East reservoir response to different reinjection scenarios and later make-up wells at the Eastern part of the field.

OW-8 provide a long history of pressure trends in the Olkaria East field from 1979. Due to pressure decline and critical assessment of pressure performance at Olkaria East, OW-8 was utilized from the year 2000 as a monitoring well. The pressure recovery as observed at OW-8 occurred from the onset of water reinjection in the 2000s. Therefore, observation from OW-8 was used to present the results of the case studies. Hot water reinjection provides fluid that elevates the pressure and supports infield productivity. Converting steam-depleted wells into reinjection wells provides chances for pressure recovery but a caution for cold inflow. Measured pressure behaviour at 800m depth (1141 masl) indicates turbulent inflow which causes drastic changes in reservoir pressures. Simulated results observed at 1200masl (Fig. 22) portrayed different responses following the case study parameters. Initial reinjection into two-phase liquid-dominated multiple reservoir zones triggers drastic linear pressure drawdown for short period. The second period occurs when is an exponentially decline and the third period allows for pressure regeneration around the wellbore. Increasing the recharge rate into a high enthalpy reservoir enhances the heat convection within the cells allowing for pressure to reduce its decline trend and provide fluid for future extraction. Case studies where infield reinjection did not occur had kinks of pressure rebound after about one year and then linear decline which was dependent on the recharge rate and well location. Case III assumed an average of 27% extracted fluid is reinjected which indicated probable pressure behaviour at OW-8.

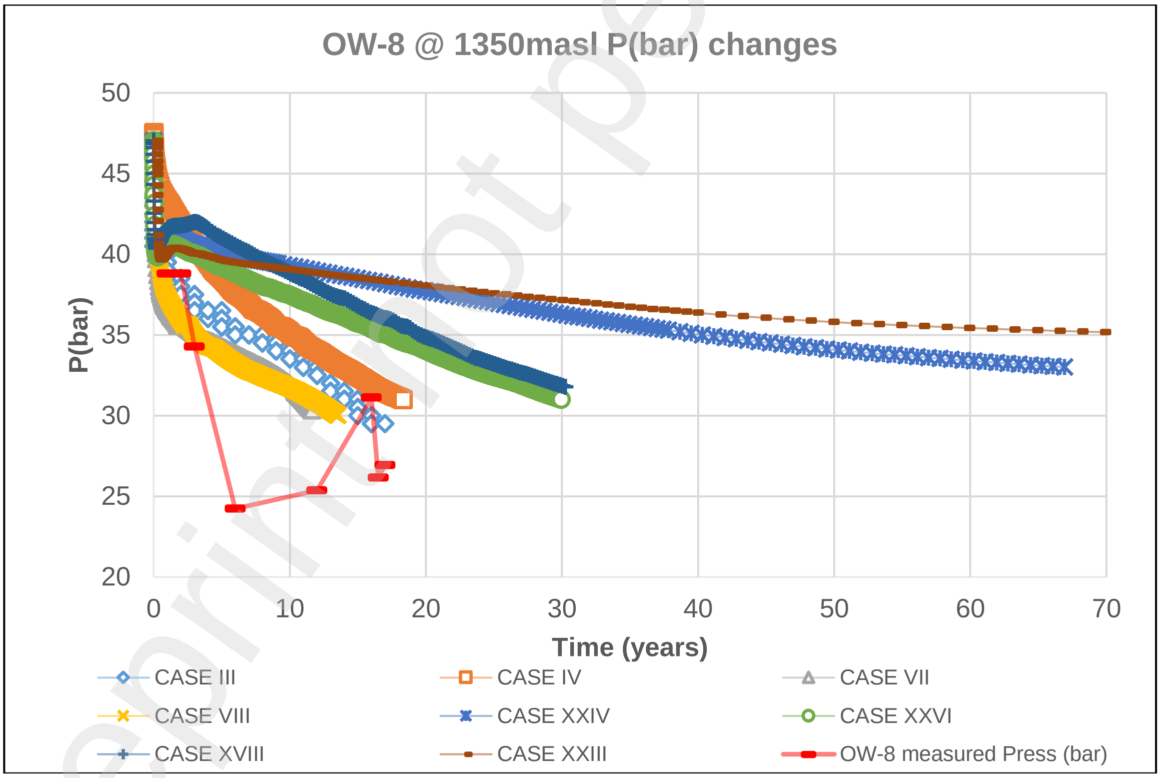

Fig. 22: Pressure change at 1200masl

The pressure observed at the trachytic intermediate reservoir at 800masl (Fig. 23) gradually declines in the same trend as the shallow reservoir. The critical pressure for the wellhead discharge is set at 5bars and above.

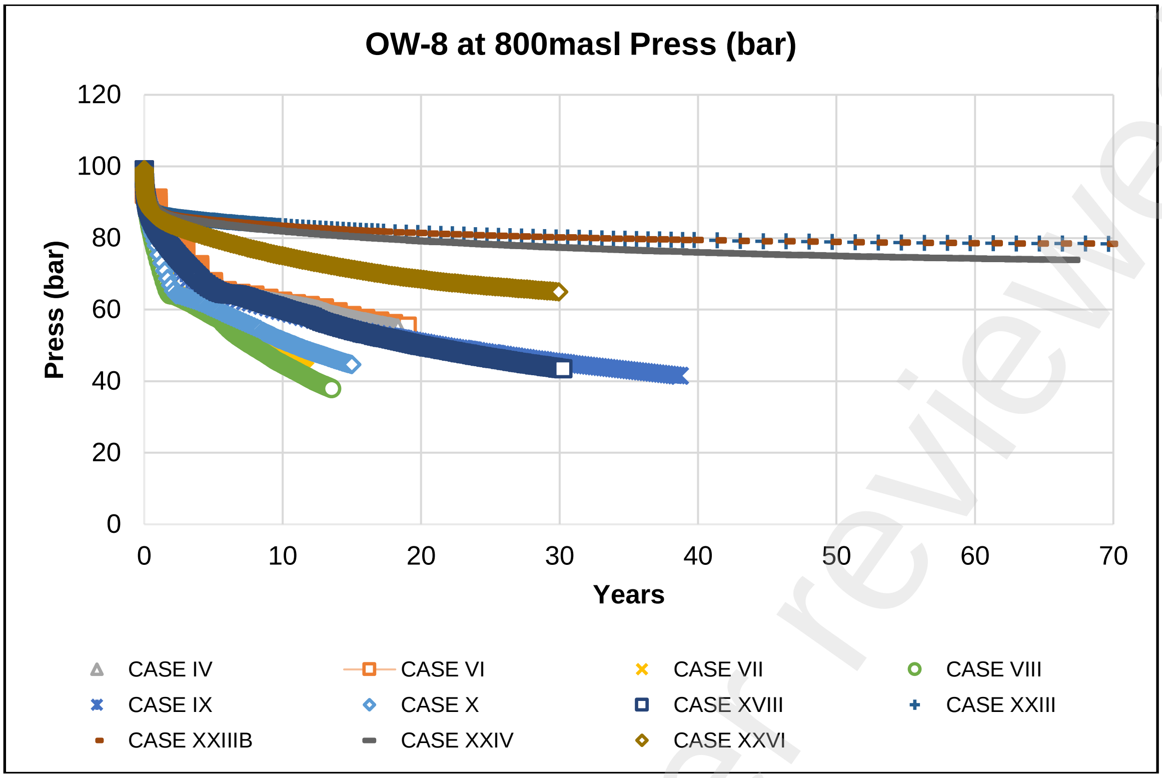

Fig. 23: Pressure change at 800masl

The interplay of the recharge rate of injected fluid, locality and depth intervals allows varied reservoir responses. At shallow and intermediate reservoirs, reinjected fluid causes pressure build-up which depends on the flow rate while overall reservoir pressure is directly influenced by the proximity of the reinjected fluid to the production zone. Fig. *24* shows the pressure profiles observed during the reinjection period in relation to the case studies assumed.

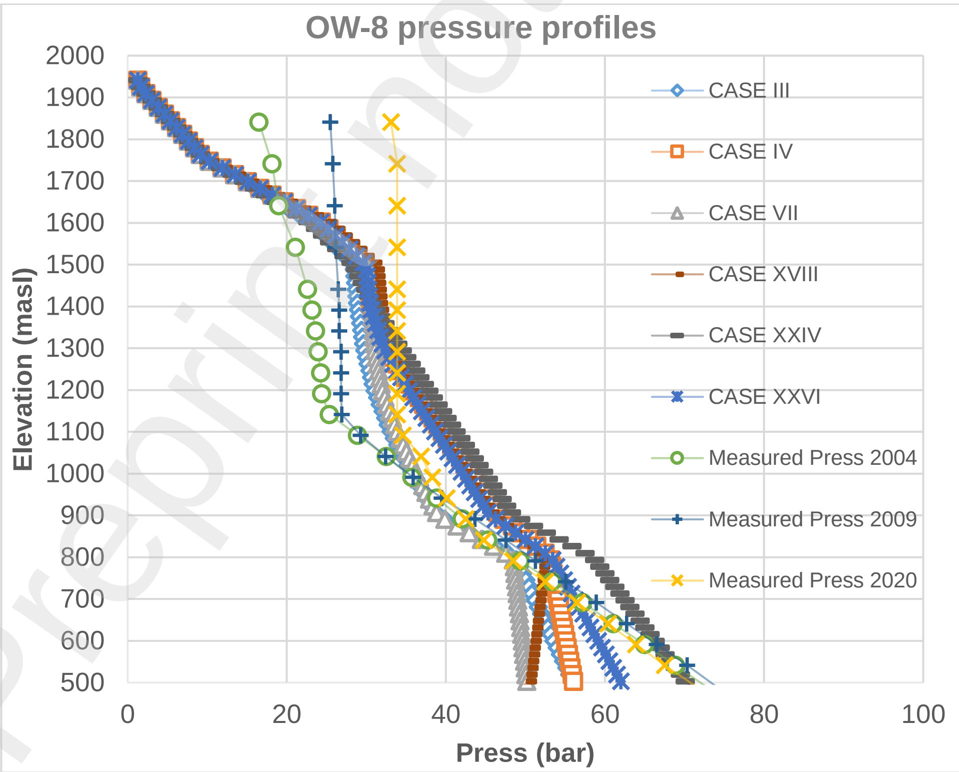

Fig. 24: OW-8 pressure profile

Major pressure change occurs at shallow and slightly at the intermediate reservoir. Deep and periphery reinjected fluid has extended pressure change to deep reservoir zones. Reservoir temperature and enthalpy decline change (Fig. 25) occurred as shown in the case studies. Increasing mass of reinjected water provides a negative effect on energy capacity but for the longevity of the project, the mass balance of fluid extraction and reinjection is necessary for project sustainability.

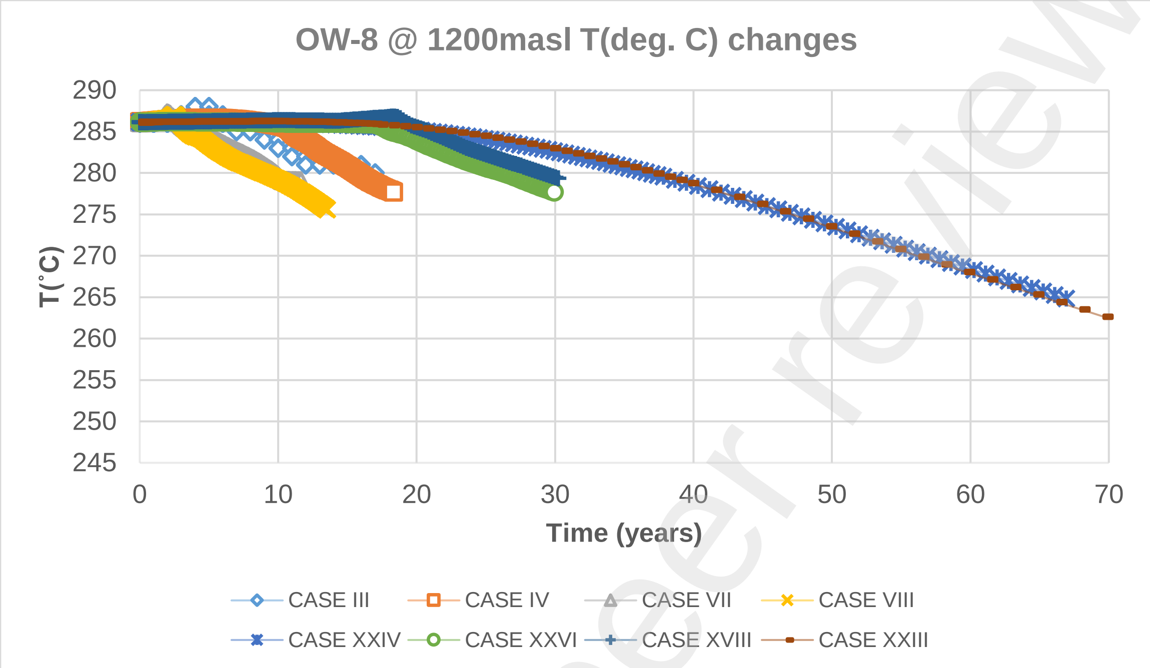

Fig. 25: Temperature change at 1200masl.

The recharge rates, well locations and recharge depth of reinjection scenarios were assessed and discussed as follows:

1) Nil reinjection program causes boiling along FLT4 which starts at OW-16 top cells shallow reservoir below caprock in the east field central zone.
2) Condensate water reinjection at OW-801 and OW-801R2 is significant for future pressure recovery but also contributes to the decline of the enthalpy, especially southeast zone. OW-17 reduced enthalpy at the shallow reservoir (central zone) which was contributed by shallow completion depth.
3) Direct reinjection of hot water at OW-7, OW-12, and OW-21 at Olkaria East central field has a direct impact on the productivity of the central zone by quick pressure change, especially at the shallow reservoir (assuming the well depth as per earlier well completion profile) while deep reservoir recovers to formation pressures and enthalpies. Gradually increasing the rate of reinjected fluid or enthalpy reduced the period for pressure and enthalpy recovery while the amount of reinjected causes pressure buildup at the shallow zones.
4) Hot water reinjection at OW-34 causes the lowest recorded enthalpies of between 674.962 - 851.760 KJ/kg.
5) Reinjection along the Ololbotut fault encourages pressure build-up west of Olkaria East field and affects adjacent wells. Its hydrothermal effect reduces to the southeast field.
6) Moving hot water reinjection to the FLT1 enhances both productivity, pressure and enthalpy recovery. Varying the rate of the

reinjection fluid along this fault has an impact on pressure build-up at the shallow reservoir and the production life of the geothermal field.

7) Deepening of hot water reinjection wells to the deep reservoir (between 500masl and 0masl) increases thermal and pressure recovery at both reservoirs. However, routine reservoir monitoring should be carried out to avoid the cooling of the deep reservoir.
8) However, re-use of hot water reinjection wells for production is possible in the central zone. The study allowed production at previously recorded rates at OW-6, OW-7, OW-12, OW-13, and OW-21 but OW-12 and OW-34 should be maintained as hot reinjection wells at a flow rate of about 36t/hr. It is important to allow for periphery reinjection, especially at the southeast field.
9) East of Ololbotut fault has shown by OW-49 (along FLT5) indicate the influence of the cold incursion and recorded minimal response to pressure changes in the reservoir sections. Therefore, this study does not recommend an extension of the field to the west of the Ololbotut fault but north of FLT5 and around FLT3.

4. CONCLUSIONS

Olkaria geothermal complex is synonymous with huge expansion supported by subsurface heterogenous fault networks and permeable reservoir rocks that guide two-phase non-isothermal fluid. This study provides a review of the geophysical parameters controlling the hydrothermal flow targeting the changes in the reservoir due to production and later reinjection strategies. Numerical analysis of the fields discovered notable high enthalpy fluid flow that is associated with highly permeable fault structures. Therefore, the southeast field has a colder region due to lateral migration of hydrothermal fluid along the lithological contacts compared to the East field faults that quickly guide its upward movement. The shallow trachytic and rhyolitic reservoir is the main source of hotter fluid for SE, which is also enhanced by sealing caprock that minimizes upward flow. Fluid-rock interaction also contributes to the loss of conductive heat flux from the heat recharge region beneath the East field.

Analytical assessment of reservoir physical properties was critical in understanding the influence of fluid-rock thermal interaction and reducing the ambiguity involved in the trial-and-error approach. Further assessment is considered owing to crosscutting permeable faults that enhance fluid exchanges in the Olkaria complex. This interconnectivity may affect the productivity of fields including the southeast field and the Domes field. The hot and condensate water reinjection case studies proposed reinjection of 1530 t/hr (73.62% of extracted fluid) south of Olkaria east field to mitigate pressure decline. Deep reinjection is important for high enthalpy fluid and reservoir productivity but caution is necessary against cooling.

Nomenclature:

R_a	Rayleigh number
g	gravity acceleration
β	Fluid thermal expansivity
ρ_w	Fluid density
C_w	Fluid compressibility
k	Permeability of porous media
h	Depth interval
ΔT	Temperature change
V_w	Specific volume
λ	Fluid viscosity
$P_{(z)}$	Pressure gradient
P	Pressure
z	Well depth (interval)
z_0	Initial depth
ρ_{sat}	Saturated fluid density
b	Open fracture

Acknowledgement: This study was supported by Japan Science and Technology (JST) and Japan International Cooperation Agency (JICA) through "Comprehensive Solutions for Optimum Development of Geothermal Systems in East African Rift Valley" (LENGO Project) by the Science and Technology Research Partnership for Sustainable Development (SATREPS) and the KIZUNA program by JICA.

REFERENCES

[1] J. K. Mulwa, F. Kimata, S. Suzuki, and Z. N. Kuria, "The seismicity in Kenya (East Africa) for the period 1906-2010: A review," *J. African Earth Sci.*, vol. 89, pp. 72–78, 2014, doi: 10.1016/j.jafrearsci.2013.10.008.

[2] N. O. Mariita, "Application of Geophysics To Geothermal Energy Exploration and Monitoring of Its Exploitation," *Short course V Explor. Geotherm. Resour.*, pp. 1–9, 2009.

[3] Cornel O. Ofwona, "Resource Assessment of Olkaria I Geothermal Field , Kenya," in *Proceedings World Geothermal Congress*, 2005, no. April, pp. 1–5.

[4] P. A. Omenda, "The geology and structural controls of the Olkaria geothermal system, Kenya," *Geothermics*, vol. 27, no. 1, pp. 55–74, Feb. 1998, doi: 10.1016/S0375-6505(97)00028-X.

[5] C. W. Karingithi, S. Arnórsson, and K. Gródienvold, "Processes controlling aquifer fluid compositions in the Olkaria geothermal system, Kenya," *J. Volcanol. Geotherm. Res.*, vol. 196, no. 1–2, pp. 57–76, Sep. 2010, doi: 10.1016/j.jvolgeores.2010.07.008.

[6] M. M. Mwania, "Evaluation of subsurface structures using hydrothermal alteration mineralogy- A case study of olkaria south east field," in *Transactions - Geothermal Resources Council*, 2015, vol. 39, pp. 559–566.

[7] E. R. Ngetich, "Mapping of Olkaria Intrusives by Integration of Geologic and Geophysical Techniques," in *Proceedings Geothermal Workshop*, 2018, vol. 43.

[8] Kengen, "Geochemical report for the Olkaria Geothermal Complex. Unpublished report," 2014.

[9] P. Ouma, V. Koech, and F. Mwarania, "Olkaria Geothermal Field Reservoir Response After 35 Years of Production (1981 – 2016)," 2016, vol. 6, no. November, pp. 1–13.

[10] A. Franco and M. Vaccaro, "Numerical simulation of geothermal reservoirs for the sustainable design of energy plants: A review," *Renew. Sustain. Energy Rev.*, vol. 30, pp. 987–1002, Feb. 2014, doi: 10.1016/J.RSER.2013.11.041.

[11] E. Wafula, "Geochemical changes and processes in the Olkaria East Reservoir 1984 to 2017," in *Proceedings, 7th African Rift Geothermal Conference*, 2018, no. November.

[12] Z. Kamila, E. Kaya, and S. J. Zarrouk, "Reinjection in geothermal fields: An updated worldwide review 2020," *Geothermics*, vol. 89, pp. 375–6505, 2021, doi: 10.1016/j.geothermics.2020.101970.

[13] B. Wang'ombe, E. Okiambe, P. Omenda, I. V. S. Rathore, and W. Ambusso, "A numerical solution to estimate hydro-geologic parameters of a fractured geothermal porous medium based on fluorescein thermal decay correction," *Geothermics*, vol. 51, pp. 124–129, 2014, doi: 10.1016/j.geothermics.2013.11.003.

[14] B. Wang'ombe, E. Okiambe, P. Omenda, I. V. S. Rathore, and W. Ambusso, "A numerical solution to estimate hydro-geologic parameters of a fractured geothermal porous medium based on fluorescein thermal decay correction," *Geothermics*, vol. 51, pp. 124–129, Jul. 2014, doi: 10.1016/j.geothermics.2013.11.003.

[15] M. J. O'Sullivan, K. Pruess, and M. J. Lippmann, "State of the art geothermal reservoir simulation," *Geothermics*, vol. 30, no. 4, pp. 395–429, Aug. 2001, doi: 10.1016/S0375-6505(01)00005-0.

[16] K. Pruess, C. Oldenburg, and G. Moridis, "TOUGH2 USER'S GUIDE, VERSION 2.0," 1999.

[17] D. Saitet, "Synthesis of Well Test Data and Modelling of Olkaria South East Production Field," in *World Geothermal Congress 2015*, 2015, no. April, p. 11.

[18] E. Rop, H. Fujii, and S. Jalilinasrabady, "An updated numerical model of the Greater Olkaria geothermal system, Kenya," in *43rd Workshop on Geothermal Reservoir Engineering, Stanford University, Stanford, California*, 2018, no. SGP-TR-213, pp. 1–13.

[19] M. L. Sorey, "Numerical modeling of liquid geothermal systems," *Prof. Pap.*, 1978, doi: 10.3133/PP1044D.

[20] R. N. Horne and M. J. O'Sullivan, "Convection in Porous Medium Heated from Below: The Effect of Temperature Dependent Viscosity and Thermal Expansion Coefficient," *Am. Soc. Mech. Eng.*, no. 77-HT-56, 1977.

[21] M. Hanano, "Two different roles of fractures in geothermal development," *Proc. World Geotherm. Congr. 2000*, pp. 2597–2602, 2000.

[22] P. W. Huang and F. Wellmann, "An Explanation to the Nusselt–Rayleigh Discrepancy in Naturally Convected Porous Media," *Transp. Porous Media*, vol. 137, no. 1, pp. 195–214, 2021, doi: 10.1007/s11242-021-01556-8.

[23] P. A. Witherspoon, C. H. Amick, J. E. Gale, and K. Iwai, "Observations of a potential size effect in experimental determination of the hydraulic properties of fractures," *Water Resour. Res.*, vol. 15, no. 5, pp. 1142–1146, 1979, doi: 10.1029/WR015I005P01142.